CONSTRUCTION OF A PULSED SUPERHETERODYNE EPR SPECTOMETER

by

Homer S. Nakayama

UNITED STATES
NAVAL POSTGRADUATE SCHOOL

THESIS

CONSTRUCTION OF A PULSED

SUPERHETERODYNE EPR SPECTROMETER

by

Homer S. Nakayama

June 1968

[redacted]

CONSTRUCTION OF A PULSED

SUPERHETERODYNE EPR SPECTROMETER

by

Homer Shiro Nakayama
Lieutenant, United States Navy
B.S., University of Oklahoma, 1962

[redacted]

Submitted in partial fulfillment of the
requirements for the degree of

MASTER OF SCIENCE IN PHYSICS

from the

NAVAL POSTGRADUATE SCHOOL
June 1968

ABSTRACT

The general theory of electron paramagnetic resonance (EPR) is discussed to present a background for the Bloch equations, hence explaining the phenomena of relaxation times in paramagnetic materials. Then, the details of construction of the pulsed superheterodyne EPR spectrometer are discussed in which the characteristics and functions of the components are specified. Procedures for its use in the measurement of T_1 are indicated and waveforms from various locations are presented to show the limitation of the pulsed EPR spectrometer that was constructed.

TABLE OF CONTENTS

LIST OF ILLUSTRATIONS

ACKNOWLEDGEMENTS

The author expresses his appreciation for the guidance, encouragement, and assistance given by Professor Gordon E. Schacher of the Naval Postgraduate School. The author also thanks Mr. Ross Seeley, for the technical assistance on the various aspects of equipment alignment and calibration, and Knotts, ET2, who loaned the author several microwave components for the pulsed EPR spectrometer.

CHAPTER I

INTRODUCTION

The purpose of building the pulsed electron paramagnetic spectrometer is to measure relaxation times of various materials. Basically, the spectrometer consists of a microwave source, resonant cavity, microwave bridge, receiver, and a device to control the amount of microwave energy to the cavity. Our spectrometer was constructed for specific measurements of the spin-lattice relaxation times or T_1. In general, these relaxation times are characteristic of the coupling of magnetization with its surrounding. There are two basic processes that are associated with these couplings, one being the spin lattice interaction that is associated with longitudinal relaxation and the other being the spin-spin interactions and inhomogeneities that are associated with transverse relaxation. The general technique employed consists of measuring transient responses of spin systems by pulse techniques. Basically, this means, (1) exposing the sample to a very high-power, short duration pulse of microwave energy, and (2) measuring the recovery rate of the induced magnetization.

First, we illustrate the origins of paramagnetism by using the iron group and rare earth elements as examples. Next, a classical theory of magnetic resonance is presented, which leads directly to the Bloch equations when quantum results are inserted at certain points to clarify the relaxation processes (spin-lattice relaxation designated T_1 and spin-spin relaxation designated T_2).

Chapter III is devoted to the discussion of the components for the pulsed electron paramagnetic resonance spectrometer that was built. Here, we categorize each major component and give a detailed discussion of its function and characteristics.

In the final chapter, the technique of operating the pulsed electron paramagnetic resonance spectrometer is presented. To show the limitation and capability for measuring T_1, the signal waveform from various sites along the system is shown.

CHAPTER II

MAGNETIC RESONANCE

The purpose of this chapter is to illustrate the principles of magnetic resonance. It is divided into three sections, starting with some examples of materials that contain paramagnetic spins. The second section presents the classical theory of magnetic resonance. Finally, in the last section, the development of the Bloch equations is presented.

I. EXAMPLES OF MAGNETIC MATERIALS

The magnetic moment of rare earth's and transition metals can be analyzed adequately if we assume only spin orbit coupling (L-S) with a Lande' g factor given by: [1]

$$g = 1 + \frac{J(J+1) + S(S+1) - L(L-1)}{2J(J+1)}$$

By Hund's rule, $\vec{J} = \vec{L} + \vec{S}$ where $\vec{J}$ is the total angular momentum vector. $\vec{S}$ and $\vec{L}$ are known as the spin and orbital angular momentum vectors respectively whose magnitudes are given by:

$$|\vec{S}| = (s(s+1))^{\frac{1}{2}}\,\hbar,$$

and

$$|\vec{L}| = (\ell(\ell+1))^{\frac{1}{2}}\,\hbar,$$

where s is the spin quantum number and ℓ is the orbital angular momentum quantum number. [2] For the rare earth's, if we let

$$\mu_{eff} = g(J(J+1))^{\frac{1}{2}} \quad ,$$

this agrees quite well with experimental values of μ_{eff}. However, the iron group yields values for μ_{eff} that are closely related to

$$\mu_{eff} = 2(S(S+1))^{\frac{1}{2}} \quad ,$$

where the value of 2 comes from considering spin only for the calculation of g. [1]

These examples are not presented to imply that the rare earth and iron groups are the only substances that exhibit paramagnetic properties but serve to illustrate some factors that cause paramagnetism. Other categories of paramagnets include triplet state molecules, stable free radicals, donors, acceptors and other impurities in solids. Because the electrons gained or lost by the impurities may be associated with an energy band of the crystal, the impurity solids are similar in nature to odd electron molecules. [3]

II. CLASSICAL THEORY OF MAGNETIC RESONANCE

Let $\vec{\mu}$ be the total paramagnetic moment for an atom arising from all contributions. Let E_i be the interaction energy of the i^{th} paramagnetic center with the magnetic field $\vec{H}_i$ in which it resides. The relationship for the interaction energy of $\vec{\mu}$ in the magnetic field is

$$E_i = -\vec{\mu}_i \cdot \vec{H}_i \ .$$

Since the field $\vec{H}_i$ may arise from the neighboring paramagnets as well as the applied field, one must treat this as a many body problem in which the paramagnets are at least coupled in pairs through magnetic dipole interactions. A great simplification results if we assume the magnetic moments are decoupled, i.e., there are no interactions and each magnetic moment may be treated independently. Then, each paramagnet has a moment $\vec{\mu}$ proportional to the total angular momentum, $\vec{J}$, of the ion/molecule and when placed in a uniform field $\vec{H}_o$, will have a ladder of $2J + 1$ evenly spaced energy levels. Thermal excitations lift fractions of the total number of these paramagnets into the upper levels and classical Boltzmann statistics predict the

resulting magnetism. [1] Unfortunately, magnetic resonance experiments cannot be adequately explained by a single particle model or uniformly spaced energy levels. Therefore, many of the studies in magnetic resonance consist of treating interacting particles by perturbation processes designed to handle weak coupling. Even weak coupling may not be readily accounted for in a many particle problem.

We now present a simplified classical description of motion of a magnetic moment in an external magnetic field, $\vec{H}$, where $\vec{H}$ may be a function of time. $\vec{H}$ will produce a torque on the magnetic moment $\vec{\mu}$ given by:

$$\vec{\tau} = \vec{\mu} \times \vec{H} .$$

If we picture a bar magnet in a constant field, the magnet will oscillate about an equilibrium position and if friction is present, the magnet will eventually align with the field and remain stationary. When the magnet possesses angular momentum, the situation is modified since it acts as a gyroscope. In the event of no friction, the moment would remain at a fixed angle with respect to $\vec{H}$, if $\vec{H}$ is constant, but the moment vector would precess about $\vec{H}$. Again, if friction forces were present, the magnet would eventually align parallel to the field. (The time the alignment would take to occur is analogous to the relaxation time T_1 see section III.)

The equation of motion for a magnet possessing angular momentum is

$$\vec{\tau} = d\vec{J}/dt = \vec{\mu} \times \vec{H} ,$$

where $\vec{\mu} = \gamma\vec{J}$ and γ is the gyromagnetic ratio. [4] Then,

$$d\vec{J}/dt = d(\vec{\mu}/\gamma)dt ,$$

and

$$d\vec{\mu}/dt = \vec{\mu} \times \gamma\vec{H} .$$

Note that this equation holds regardless of whether or not $\vec{H}$ is time dependent and that any time dependent changes in $\vec{\mu}$ are perpendicular to both $\vec{H}$ and $\vec{\mu}$. We see that $\vec{\mu}$ precesses about $\vec{H}$ with a precessional velocity given by

$$\vec{\omega}_p = \gamma\vec{H}.$$

Now convert to a co-ordinate system rotating with angular frequency Ω. Assume $\Omega \neq \omega_p$ and let $d\hat{i}/dt = d_t\hat{i}$. Then, in general

$$d_t\hat{i}' = \Omega \times \hat{i} ,$$

where $\hat{i}'$ is the rotating co-ordinate unit vector. Now write

$$\vec{\mu} = \mu_1\hat{i}'_1 + \mu_2\hat{i}'_2 + \mu_3\hat{i}'_3 ,$$

where μ_i's are components along the 1,2,3 axes and the $\hat{i}_i$'s are the corresponding unit vectors. Then,

$$d_t\vec{\mu} = \sum_j \hat{i}'_j d_t\mu_j + \sum_j \mu_j d_t\hat{i}'_j$$

$$= \sum_j [\hat{i}'_j d_t\mu_j + \Omega \times (\hat{i}'_j\mu_j)] .$$

Define,

$$\sum \hat{i}'_j d_t\mu_j = d'_t\vec{\mu} ,$$

which is the time derivative with respect to the rotating co-ordinate system. Then,

$$d_t\vec{\mu} = d'_t\vec{\mu} + \vec{\Omega}\times\vec{\mu},$$

or

$$d_t\vec{\mu} = \vec{\mu} \times \gamma\vec{H} = d'_t\vec{\mu} + \vec{\Omega} \times \vec{\mu} .$$

Hence,

$$d'_t\vec{\mu} = \vec{\mu} \times (\gamma\vec{H} + \vec{\Omega}) .$$

If we say that an effective field can be defined in terms of $\vec{H}$ and $\vec{\Omega}$ as $\vec{H}_{eff} = \vec{H} + \vec{\Omega}/\gamma$, we have,

$$d'_t\vec{\mu} = \vec{\mu} \times \gamma\vec{H}_{eff} .$$

Note that $\gamma\vec{H}_{eff}$ is the precessional rate with respect to the rotating co-ordinate system. Now, if $\vec{H} = H_o\hat{k}$ and we choose $\vec{\Omega} = -\gamma H_o\hat{k}$, $= \omega_o\hat{k}$, where ω_o is the precessional rate of $\vec{\mu}$ in the laboratory co-ordinate system, then,

$$d'_t\vec{\mu} = 0 ,$$

meaning that $\vec{\mu}$ is stationary in this rotating co-ordinate system, as one would expect. This concept is most useful in defining an effective field, H_{eff}, in a rotating co-ordinate system, which will have application in what follows.

Say in addition to $\vec{H}_o$ we have an alternating field, $\vec{H}_1$, applied perpendicular to $\vec{H}_o$ ($H_1 << H_o$). The effect of this alternating field is most readily seen if the field is broken into two components, each of amplitude H_1, rotating in opposite directions about $\vec{H}_o$.

ALTERNATING FIELD, H_1

Figure 2-1

Since one component is rotating in the same sense as the precession of the moment, $\vec{\mu}$, and one in the opposite sense, neglect the component that is counter-rotating, since it has no net effect on $\vec{\mu}$.

For ease of computation we now transform to a co-ordinate system rotating with angular frequency equal to the rotational rate of H_1;

$$\vec{H}_1 = H_1(\hat{i}\cos\Omega t + \hat{j}\sin\Omega t), \text{ (stationary co-ordinate system)}$$

$$\vec{H}_1 = \hat{i}'H_i, \text{ (rotating co-ordinate system)}$$

and

$$d\vec{\mu}/dt = \gamma\vec{\mu}X\ (\vec{H}_o + \vec{H}_1).$$

In the rotating co-ordinate system,

$$d'_t\ \vec{\mu} = \gamma\vec{\mu}\ X\ [(\vec{H}_o - \Omega/\gamma\ )\hat{k} + H_1\hat{i}']$$

$$= \gamma\vec{\mu}\ X\ \vec{H}_{eff},$$

where

$$\vec{H}_{eff} = (H_o - \Omega/\gamma)\hat{k} + H_1\hat{i}'$$

is the effective field in the rotating frame of reference.

Note that three cases can occur:

(1) $\Omega = \omega_o$ implies that $\vec{H}_{eff} = \vec{H}_1$ and the precession about $\vec{H}_1$ is $\vec{\omega}_1 = \gamma\vec{H}_1$.

(2) $\Omega << \omega_o$ implies that the magnetization vector precesses in loops.

(3) $\Omega >> \omega_o$ implies that the magnetization vector precesses with nutations.

If H_o is greater than Ω/γ, $\vec{H}_{eff}$ lies in the positive $\hat{k}$ direction and if H_o is less than Ω/γ, $\vec{H}_{eff}$ lies in the negative $\hat{k}$

direction. For the resonance condition $\vec{H}_o = \vec{\Omega}/\gamma$, and the effective field is just $\vec{H}_1$. Then a magnetic moment that is initially parallel to the static field, $\vec{H}_o$, will precess about $\vec{H}_1$, remaining perpendicular to $\vec{H}_1$, and periodically becoming perpendicular, anti-parallel, perpendicular, and parallel to $\vec{H}_o$.

Now, if $\vec{H}_1$ is applied for a short duration, t_w, the moment, $\vec{\mu}$, will precess through an angle $\theta = \gamma H_1 t_w$. If t_w were chosen such that $\theta = \pi$, the pulse of $\vec{H}_1$ would invert the moment, i.e., take $\vec{\mu}$ from being parallel to $\vec{H}_o$ to being anti-parallel to $\vec{H}_o$. Similarily, if t_w were such that $\theta = \pi/2$, the magnetic moment would become perpendicular to $\vec{H}_o$ and then precess about $\vec{H}_o$ in this orientation after removal of the $\vec{H}_1$ pulse. This leads to a simple method of observing resonances. Place the sample in a coil that is perpendicular to the static field $\vec{H}_o$ and apply $\vec{H}_1$ for a short time such that $\theta = \pi/2$. Then observe the resulting alternating induced EMF caused by the precession of the moment, $\vec{\mu}$, about $\vec{H}_o$. From the analysis above, this EMF persists indefinitely but in reality this is not true because the spins interact with their surroundings. Eventually this EMF will decay as the magnetic moment returns to its equilibrium position. For nuclear spins in liquids, decay times are on the order of several milliseconds while solids exhibit decay times on the order of 100 microseconds. [4] Decay times for electron spins are ordinarily much shorter.

Now, for a different type of observation of magnetic resonance, assume a sample containing magnetic moments is placed in an external magnetic field $\vec{H}_o$ and enclosed in a single coil (nuclear magnetic resonance, NMR) or microwave cavity (electron paramagnetic resonance, EPR) which produces the alternating field, $\vec{H}_1$. If $\vec{\Omega} = \vec{\omega}_o$, then energy will be absorbed from the $\vec{H}_1$ field to tip the magnetic moments,

$\vec{\mu}$, away from their equilibrium positions. This absorption of energy will be evidenced by a change in the Q of the coil or microwave cavity which is easily measured experimentally. If all spins in the sample were in the same field, an infinitely sharp resonance line would be observed at the resonance frequency $\omega_o/2\pi$. However, due to inhomogeneities in $\vec{H}_o$, the sample, and other interactions, the observed resonance line has a non-zero width whose shape is often Lorentzian or Gaussian. [4]

III. BLOCH EQUATIONS

In Bloch's pioneering work on nuclear magnetic resonance, he developed a set of equations to describe the dynamic behavior of the macroscopic magnetization in a nuclear paramagnetic material. These equations are equally useful for understanding electronic or ferromagnetic resonance. The Bloch equations apply most directly to two level spin systems, but are useful in multilevel systems if their limitations are not exceeded. The derivation utilizes a classical analysis where some quantum results are inserted at certain points to clarify the relaxation process. We proceed to first discuss the relaxation processes.

For the case of spin-lattice interactions, this is thought of as an energy transfer from the spin system to the lattice. [3] The nature of this phenomena is thermal. The thermal fluctuations most responsible for the relaxation transistions are the thermal vibrations of the crystal lattice. When a spin makes a relaxation transition in one direction or another, it simultaneously exchanges a quantum of energy with the lattice thermal vibrations. These thermal vibrations in the crystal are equivalent to thermally excited sound waves or

lattice vibrations running through the crystal. The frequencies of these sound waves cover the spectrum from zero to frequencies characteristic of infrared radiation. One quantum of lattice vibration is commonly called a phonon, in analogy to a photon of electromagnetic energy. The Planck relationship of $E = hf$ holds equally well for phonons as for photons; therefore, when a spin relaxes, it can be viewed as absorbing or emitting one phonon of lattice energy at the transition frequency, $f = \Delta E/h$, where ΔE is the change in the spin's energy between a final state, E_2, and an initial state, E_1.

The rates that transitions occur can be given by upward and downward relaxation transition probabilities, w_{12} and w_{21} per spin per unit time. The probability, w_{12}, is defined as the probability per unit time that a spin in level 1 will make a relaxation transition to level 2. The total number of upward transitions per unit time is then $w_{12}n_1$ where n_1 is the number of spins in level 1. Similarly, the total number of downward transitions are $w_{21}n_2$. The magnitudes of w_{12} and w_{21} are related to the magnitude of thermal vibrations in the surroundings and the degree of coupling between the spins and their surroundings.

The relaxation rate equations governing the time rate of change of the level populations, n_1 and n_2, are

$$dn_1/dt = -w_{12}n_1 + w_{21}n_2 ,$$

and

$$dn_2/dt = w_{12}n_1 - w_{21}n_2 .$$

Note that the total number of spins, N, equals $n_1 + n_2$ and the condition that $dN/dt = 0$ is satisfied (conservation of spins).

Due to the fact that the interactions with the surroundings depend on the spin states, w_{12} and w_{21} differ in magnitude. There is one fundamental requirement that must be satisfied that enables one to simply find their ratio: this is that at thermal equilibrium, the level populations must be in static equilibrium. Hence, putting $n_1 = N_1$ and $n_2 = N_2$, where N_i indicates thermal equilibrium values of n_i, into the relaxation rate equations must lead to

$$dN_1/dt = dN_2/dt = 0 \ .$$

This can occur only if the relaxation transition probabilities obey the condition

$$w_{12}/w_{21} = N_2/N_1 = \exp(-\Delta) \ ,$$

where $\Delta = (E_2 - E_1)/kT$. This implies that the downward transition probability, w_{21}, must always be larger than the upward transition probability, w_{12}, by the Boltzmann factor if thermal equilibrium is to be maintained.

By subtracting the second rate equation from the first, a single rate equation results for the population difference, n:

$$\begin{aligned} dn/dt &= dn_1/dt - dn_2/dt \\ &= 2(w_{21}n_2 - w_{12}n_1) \\ &= (w_{21} - w_{12})N - (w_{12} + w_{21})n. \end{aligned}$$

If the value of n is zero at time t = 0, the solution to this equation is

$$n = n_o(1-\exp(-t/T_1)) \ ,$$

where $n_o = \frac{(w_{21} - w_{12})N}{w_{12} + w_{21}}$ is the thermal equilibrium population difference and the time constant related to this mechanism is given by:

$$T_1 = (w_{12} + w_{21})^{-1} \quad .$$

This is the time constant commonly termed the spin-lattice relaxation time. Also, T_1 is sometimes called the longitudinal relaxation time since it gives the rate of change of magnetization parallel to H_o. [3]

Note that if the approximation that $\Delta << 1$ is valid, then $w_{12} \simeq w_{21}$ and $T_1 \simeq 1/2w_{12}$. Numerical values for T_1 vary over a wide range depending on the material and are commonly between 1 second and 1 microsecond. [3]

The effect of H_1 is to cause stimulated transitions, whose probabilities, W_{12} and W_{21}, are equal. The effect of an applied H_1, then, will be to tend to equalize the populations in levels 1 and 2. This can easily be shown as follows. The total number of stimulated transitions upward per unit time caused by H_1 are $W_{12}n_1$ and the corresponding downward transitions are $W_{21}n_2$. Then the rate equations become

$$dn_1/dt = -w_{12}n_1 + w_{21}n_2 - W_{12}n_1 + W_{21}n_2 \ ,$$

and

$$dn_2/dt = \ w_{12}n_1 - w_{21}n_2 + W_{12}n_1 - W_{21}n_2 \ .$$

Hence, upon subtraction of the first from the second rate equation and setting $W_{12} = W_{21} = W$ we find

$$dn/dt = (n_o - n)/T_1 - 2Wn.$$

For steady-state, $dn/dt = 0$ and we find

$$n = n_o/(1 + 2WT_1) \ .$$

Therefore, n has the following limits: $n = n_o$ for $WT_1 << 1$ and $n = 0$ for $WT_1 >> 1$. Thus a large H_1 (W large) reduces the population difference to 0, or $n_2 = n_1$.

The magnetic resonance signal is proportional to the population difference, n, since a large n will mean a greater amount of energy is absorbed from the alternating field. The induced transition probability is proportional to the incident power, thus at high incident powers, large alternating H_1 field, the magnetic resonance signal disappears. This phenomenon is called saturation.

We now develop the Bloch equation, utilizing the relaxation time discussed above. The Bloch equation for the z-component of magnetization becomes [4]

$$dM_z/dt = (M_z - M_o)/T_1 \ ,$$

where $\vec{M} = \sum \vec{\mu}_i$ is the net magnetization vector for the system given by the vector sum of the individual magnetic moments. $\vec{H}_o = H_o\hat{k}$, and, at thermal equilibrium, the net magnetization $\vec{M}_o$ is along $\vec{H}_o$ and $M_x = M_y = 0$. The above equation is written assuming $\vec{H}_1 = 0$.

It is also experimentally observed that magnetization perpendicular to H_o will decay to zero and that the time constant associated with this process is often much shorter than T_1. This relaxation rate is commonly called the spin-spin or transverse relaxation time and is designated T_2. [3]

One can immediately write the equation for the x-and y-components of magnetization as follows; [4]

$$dM_x/dt = - M_x/T_2 + (\vec{M} \times \gamma\vec{H}_o)_x \ ,$$

and

$$dM_y/dt = - M_y/T_2 + (\vec{M} \times \gamma\vec{H}_o)_y \quad .$$

A physical interpretation of the transverse relaxation process can be related directly to the line-width. Due to sample inhomogeneities (including contributions from spin-spin interactions) not all spins precess at the same rate about H_o. Thus, individual spin components perpendicular to H_o will get out of phase as time progresses and any transverse component of magnetization will decay to zero. Of course, the distribution of local fields which cause this effect is immediately apparent as a width of the magnetic resonance line. The greater this width, the shorter T_2 will be. One can show that $T_2 = 1/\gamma\Delta H$ where ΔH is the half width of the resonance line at one-half magnitude. [1]

If $\vec{H}_1 \neq 0$ then the three-component equations for $d\vec{M}/dt$ should be modified by writing $\vec{M} \times \gamma\vec{H}$ in place of $\vec{M} \times \gamma\vec{H}_o$ where $\vec{H} = \vec{H}_o + \vec{H}_1$. The presence of this additional term will modify the equilibrium values of magnetization. [1] Hence, the Bloch equations have the form, [3]

$$dM_x/dt = - M_x/T_2 + \gamma(\vec{M} \times \vec{H})_x \quad ,$$

$$dM_y/dt = - M_y/T_2 + \gamma(\vec{M} \times \vec{H})_y \quad ,$$

$$dM_z/dt = (M_o - M_z)/T_1 + \gamma(\vec{M} \times \vec{H})_z \quad .$$

These functional relationships are a result of the assumptions made. That is, at thermal equilibrium, the net magnetization vector is parallel to H_o, i.e., that the x- and y-components vanish. Also, note that the same relaxation time, T_2, was chosen for both the x- and y-directions and that it can be different from the longitudinal relaxation time, T_1. [4]

CHAPTER III

ELECTRON PARAMAGNETIC RESONANCE SPECTROMETER

In this chapter the components of the electron paramagnetic resonance spectrometer are discussed in detail. The components include the following items: (1) klystron generator, (2) isolator, (3) directional coupler, (4) variable attenuator, (5) diode switch, (6) pulse generator, (7) magic tee, (8) microwave resonant cavity, (9) crystal detector, (10) slide screw tuner, (11) wave meter, (12) thermistor, (13) microwave average power meter, (14) Varian V-4200 EPR Spectrometer, and (15) superheterodyne receiver (discussed separately in section II).

I. DISCUSSION OF THE COMPONENTS

For the generation of microwave energy, a Varian Associates V-58 klystron was chosen. The oscillation mode used is approximately 50 MHz wide with a mechanical tuning range of 8.5 GHz to 10.0 GHz. The peak power, which occurs in the center of the mode, was determined to be 610 milliwatts.

Next, a ferrite device, a Uniline X-1312 isolator was installed. This device permits unattenuated transmission but provides very high attenuation in the reverse direction. [6] This means the reflected signal from the other components of the microwave system does not get transmitted back to the generator, the klystron. Consequently, the klystron sees a matched load and effects such as power output variation and frequency change with variations in load impedance are avoided.

The directional couplers, Microline 170XC 20 db couplers, are used as microwave junctions. One is for power monitoring and the other is for a reference cavity to provide automatic frequency control (AFC).

One precision attenuator, Hewlett Packard X382A, provides the control for power level settings. The orientation of the ferrite card

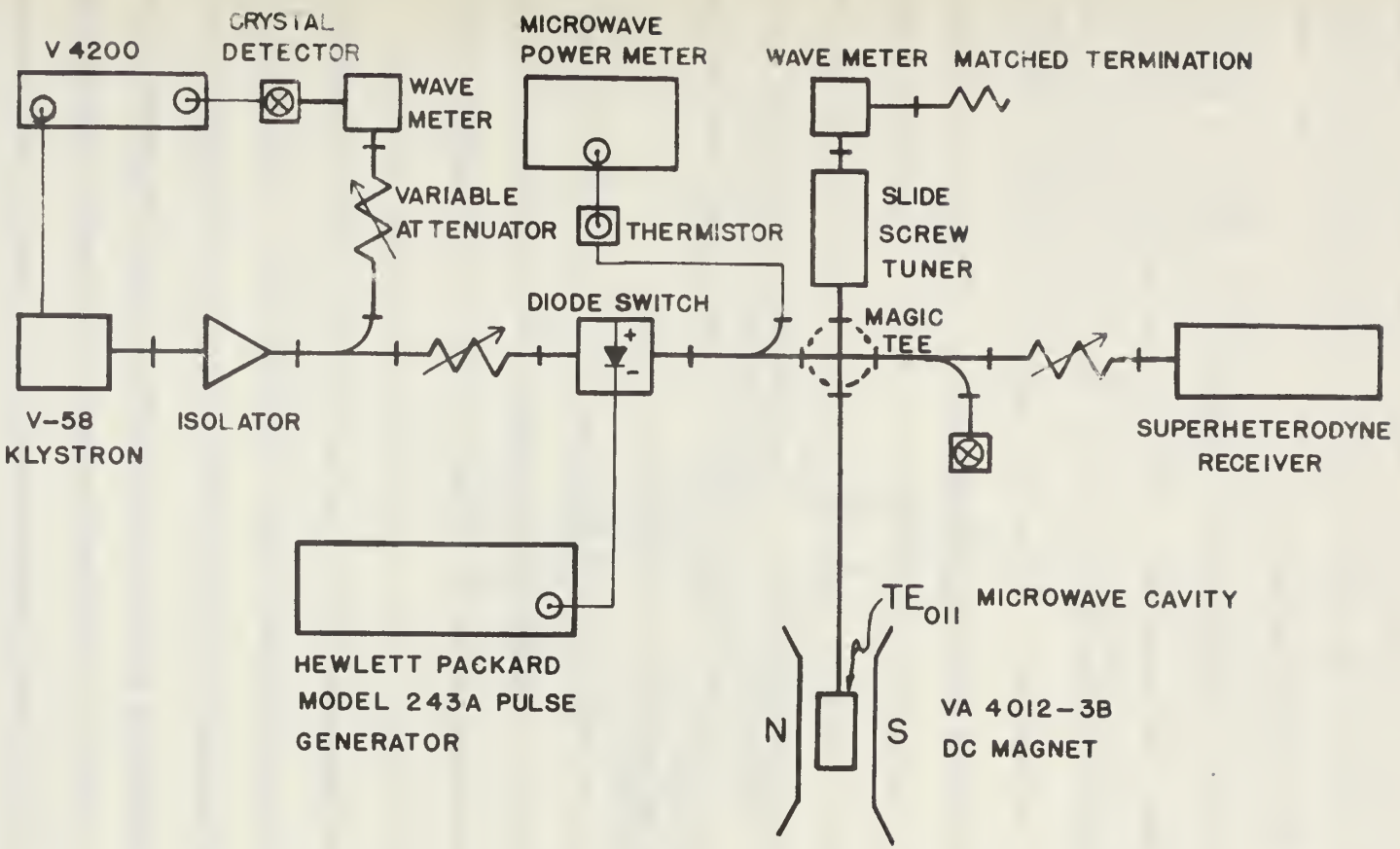

PULSED EPR SPECTROMETER

(SCHEMATIC)

Figure 3-1

in the attenuator determines the amount of attenuation that is presented to the microwave signal. [5] The remaining attenuators are Hewlett Packard X375A attenuators and serve as power limiters for the local oscillator and the EPR signal input to the balanced mixer (discussed in the Superheterodyne Section).

The diode switch, Microwaves Associates MA 8319-1X17, is a fast rise, diode element microwave gate. The internal description of this particular component is questionable since there is no literature available. A rough calibration of the switch indicated a minimum insertion loss of 1.15 db can be expected when the applied voltage is less than -10 volts and a maximum insertion loss of 37 db at +1 volt (see Figure 3-1 for polarity). However, specific values of insertion loss must be found by considering two parameters, the power that is incident on the switch and the voltage that is applied. With these relationships, the insertion loss and the diode current can be found.

To provide the switching for the diode gate, a Hewlett Packard 243A pulse generator is used. This unit is capable of outputs from dc to 0.05 microsecond pulses of either polarity at frequencies from dc to 1.0 MHz.

A principal component of the microwave bridge is the Microwaves Associates MA 541 matched magic tee. The magic tee is a four-port microwave junction such that the incident power is divided equally between two arms and no power is transmitted through the remaining arm. [5] For example, if the incident microwave power is applied to arm 1, it is divided equally between arms 2 and 3 but no power is transmitted to arm 4. (See Figure 3-2.) Arm 2 is terminated with a matched load, the characteristic impedance of the waveguide, arm 3 is connected to the microwave cavity, and arm 4 is used as the output port

that is connected to the superheterodyne receiver. This bridge is operated near a matched condition implying that when no reflected power is incident from arm 3 there is no microwave power transmitted to arm 4. Power loss by a factor of one-half, associated with each transit of microwave energy, is the disadvantage encountered when the magic tee is used for the bridge. To reiterate, one-half of the incident power from the klystron appears at the cavity and one-half of the reflected power from the cavity appears at the receiver.

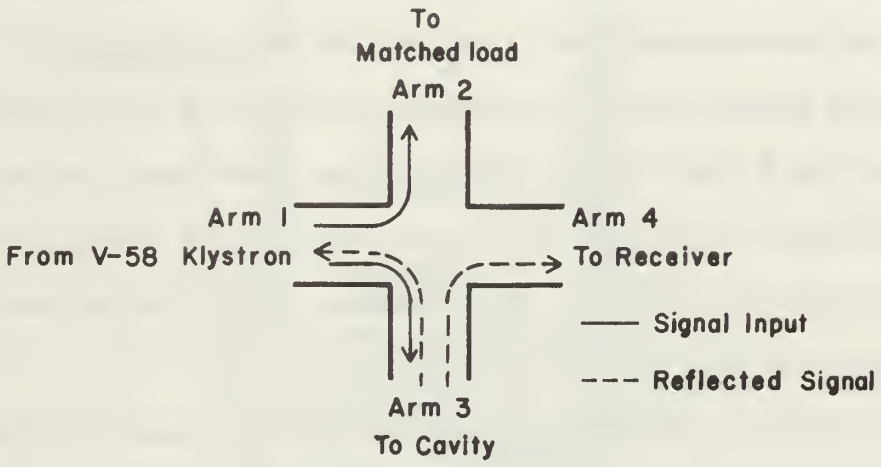

MAGIC TEE SCHEMATIC
Figure 3-2

Since the microwave resonant cavity is an important component of the EPR spectrometer, a detailed analysis of some specific properties is presented here. In essence, the resonant cavity is a box fabricated from a highly conductive metal with dimensions comparable to the microwave wavelength. [6] At resonance, the cavity is capable of sustaining microwave oscillations which form an interference pattern, or standing waves pattern, from superimposed microwaves multiply reflected from the cavity walls. Each particular cavity size and shape can sustain oscillations in a number of different standing wave configurations called

modes. When a wave guide is terminated in its characteristic impedance, Z_o, the transverse electric field and the transverse magnetic field reach a maxima at the same longitudinal position. In other words, they are in phase with each other with respect to space and time. This maximizes the time averaged Poynting's vector or the vector rate of energy flow, $\vec{P} = \frac{1}{2}\vec{E} \times \vec{H}$. [6] However, in a resonant cavity, the electromagnetic field configurations are a result of standing waves with the transverse magnetic field maximum occurring $\lambda_g/4$ from the transverse electric field maximum so they are in space quadrature. This makes Poynting's vector vanish and consequently there is no net energy flow but merely energy storage and dissipation. In resonant cavities, the wave patterns are such that the H field lines of force always form loops that enclose the E field lines of force and the E field lines either form loops which enclose the H field lines or they terminate on induced surface charges in the walls of the cavity.

The particular microwave cavity that is used here is cylindrical and oscillates in the TE_{011} mode at the desired frequency. All surfaces of the cavity are gold plated to a thickness of about 0.003 inches to increase electrical conductivity and to prevent tarnishing (Figure 3-3). Since the TE_{011} and the TM_{111} modes are degenerate at all frequencies [7], the purpose of the TM_{111} suppression step, indicated in Figure 3-3, is to eliminate this undesired mode which relies on surface currents for its existence. An analysis of the TE_{011} mode would show that there are no induced surface currents between the cylinder wall and the endplate hence the suppression step does not affect this mode. Another item of interest in Figure 3-3 is the tuning disc. This element acts as a flux steering device and appears to have lumped parameter characteristics of a capacitive-inductive tuner, similar in

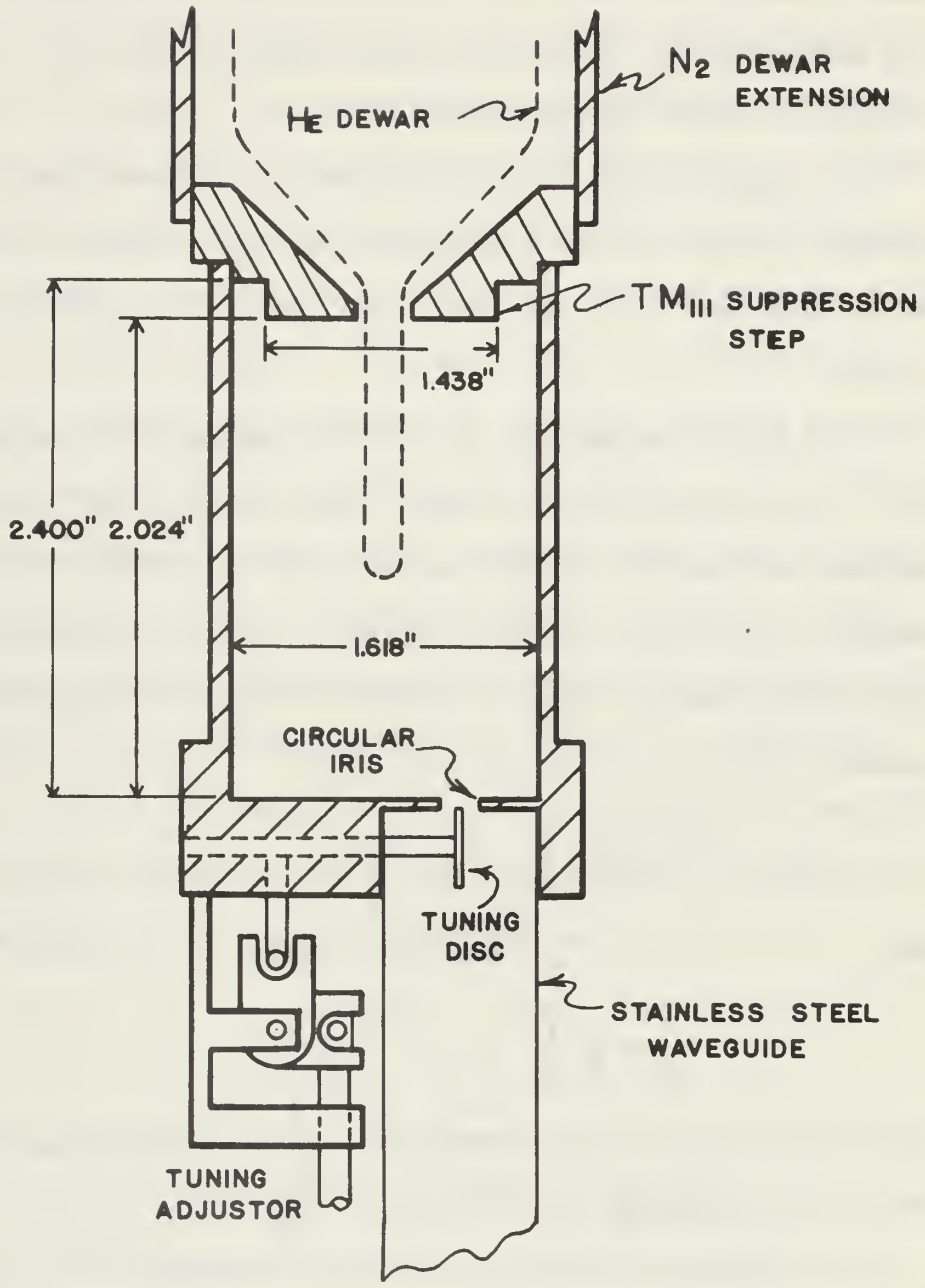

MICROWAVE RESONANT CAVITY

Figure 3-3

nature to the E-H tuner. The transverse location of the tuning disc governs the cavity coupling. The transverse positioning is accomplished by a mechanical arm connected to the tuning adjustor that protrudes through the outer dewar assembly.

The general property of a microwave cavity resonantor that is of greatest interest is the quality factor, or Q. The Q of the TE_{011} is fairly high and in our particular case the Q is calculated to be around 13,000.

In a high Q resonator, the electric and magnetic fields are 90^{o} out of time phase with each other. When the electric fields are at a maximum, the magnetic fields are zero, and vice versa. Hence the stored energy in the electric field is equal to the stored energy in the magnetic fields and the form of the expressions for the stored energy becomes [6]

$$U_E = \frac{\varepsilon}{2} \int_o^{\tau} | E_m |^2 \, dt \, ,$$

and

$$U_H = \frac{\mu}{2} \int_o^{\tau} | H_m |^2 \, dt \, .$$

Each is evaluated at the part of the cycle corresponding to the maximum value denoted by the subscript m.

The losses in a cavity arise from the dissipation of heat caused by the surface currents in the skin effect resistance and this ohmic loss is given by [6]

$$P_L = \frac{R_S}{2} \int_S |H_{tm}|^2 \, dS \, ,$$

where the maximum tangential field, H_{tm}, along the surface is integrated over all the cavity walls. There may be an additional loss

of energy due to dielectrics such as water or a paramagnetic sample with a large loss tangent. Also, there will be losses from radiation out of the cavity coupling hole; however, the losses due to the coupling hole are generally negligible. The losses due to the paramagnetic spins in the sample are the essence of magnetic resonance experiments. Thinking in terms of the earlier explanation of magnetic resonance, the change in cavity Q is related to the absorption of energy from the magnetic field by the spin system on resonance. The real part of the magnetic susceptability, χ', changes the inductance of the cavity and the imaginary part of the susceptability, χ'', modifies the resistance. [4] The real part of the susceptability represents a reactive effect that is zero on resonance and has broad peaks of opposite sign on each side of resonance, causing a frequency shift in cavity resonance that is first positive, then zero, then negative as magnetic resonance is traversed. The imaginary part of the susceptability causes a decrease in the Q of the cavity which is a maximum at the center of magnetic resonance and decreases monotonically to zero away from resonance.

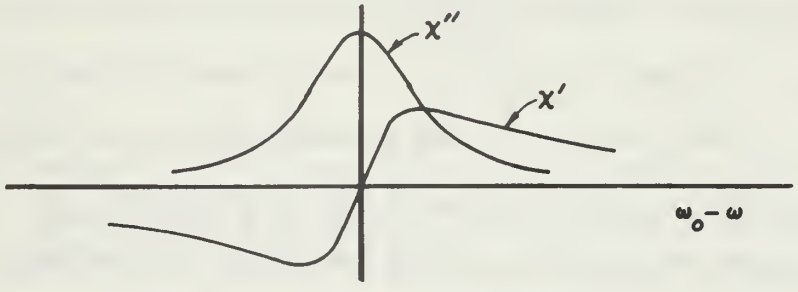

χ' AND χ'' VERSUS $\omega_0 - \omega$

Figure 3-4

A bead thermistor, Hewlett Packard 477B, in conjunction with a Sperry Microline 31A1 average power meter is used to determine input

power to the magic tee bridge. The two units, the thermistor and power meter, act as a bridge where the thermistor is one element of the bridge and the power meter contains the remaining three elements. The bead thermistor installed in this spectrometer has a nominal value of resistance of 200 ohms, requires negative bias voltage with about 13 milliamps of bias current for power measurements between 3 and 10 milliwatts, and about 16 millamps bias current for power measurements between 0.1 and 1 milliwatt. The disadvantage of using a thermistor is that since it is a semiconductor device, it is sensitive to temperature fluctuations, both ambient, and generated due to power dissipation in the thermistor bead. [7]

The crystal detectors used are all 1N23WE crystals. Two matched crystals are used in the balanced mixer (see Section II) and one crystal is used for an input to the Varian console to initially establish the location of the sample cavity resonance. The remaining crystal is used as a detector for the automatic frequency stabilization device called the pound stabilizer. [8] This device consists of the directional coupler, attenuator, wavemeter, crystal detector, and the Varian Associates console, as shown in Figure 3-1, and is used to stabilize the frequency of the V-58 klystron. The wavemeter acts as a reference cavity that is set on the desired klystron operating frequency. The crystal detector is used to convert the microwave energy to a dc signal that is fed to the console. Within the console there is a bridge network plus an amplifier that controls the reflector voltage to the V-58 klystron in the AFC mode of operation.

The most sensitive microwave bridge arrangement is when the cavity is critically coupled. When the cavity is tuned for critical coupling on resonance, as resonance is traversed the sample will change the Q

of the cavity such that the coupling goes from under-coupled to critical-coupled to over-coupled which is undesirable. [6] If we use the slide screw tuner, Hewlett Packard X870A, to introduce the proper amount of carrier signal or leakage, this effect is eliminated. The magnitude of the carrier signal is proportional to the depth of probe insertion and the location of the probe along the waveguide determines the phase of this signal. As stated earlier, at magnetic resonance, χ' and χ'' of the sample both change and the amplitude of the observed signal from χ' will be comparable to that observed from χ''. Hence the slide screw tuner is employed to vary the phase of the leakage signal so that one can set the spectrometer to be sensitive to either χ' or χ'' or a mixture of the two. However, if the klystron is stabilized on the sample resonant cavity by an AFC circuit, then the klystron will "follow" the frequency pulling of the cavity by χ' and the dispersion mode will be stabilized out. In this way an EPR spectrometer can be made to record only the absorption mode, χ''.

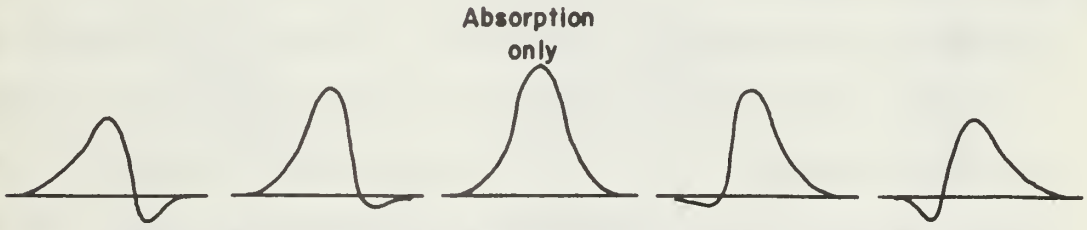

Change in shape of the observed EPR spectrum when the bridge is tuned continuously by continuous change in position of the slide-screw tuner.

Figure 3-5

The final component, the Varian Associates V4200 NMR spectrometer, modified with a Varian Associates V4500-10A EPR control unit is used for the V-58 klystron power supply and for AFC for the klystron generator.

As stated earlier, this section of the console contains the bridge circuit and amplifier for the Pound Stabilizer. The instruction manual for the EPR spectrometer [9] gives a detailed description of the circuitry hence it will not be discussed here.

II. SUPERHETERODYNE SYSTEM

The superheterodyne receiver is probably the most common receiver employed today. It finds application in almost all radios and most radars. The superheterodyne receiver beats the input signal with a local oscillator to produce a difference signal, or an intermediate frequency (i.f.). In most microwave applications, this difference frequency is 30, 60, or 90 MHz. The major advantage of this type of receiver is crystal noise reduction. [10]

For the spectrometer that was constructed, the superheterodyne receiver consists of five components which are described below:

(1) Balanced mixer: The balanced mixer, Microwaves Associates MA 810, is used to balance out local oscillator noise at the input to the mixer-preamplifier. The operation of this unit can be best visualized by referring to a magic tee. Visualize two microwave crystal diodes located on arms 2 and 3 of the magic tee (refer to Figure 3-2 for arm numbers). The local oscillator signal is applied to the H-plane arm, arm 4, and will arrive at the diodes in phase. The EPR signal is fed into the E-plane arm, arm 1, and will arrive at the diodes out of phase. The difference frequency signal, produced by the mixing of the local oscillator with the EPR signal in the non-linear diodes will be 180° out of phase while the local oscillator noise will be in phase. By connecting the diode outputs to a balanced amplifier, push-pull arrangement, the local oscillator noise is seen to cancel while the difference signals add in phase. Another advantage obtained

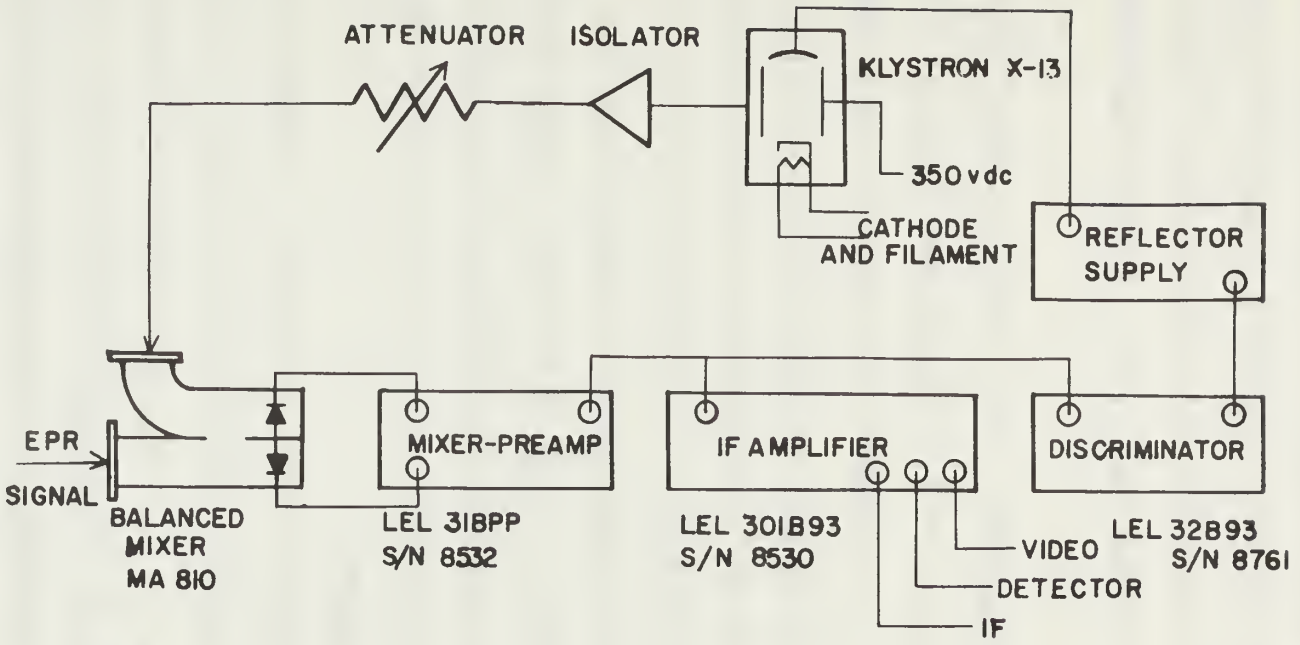

SUPERHETERODYNE RECEIVER

(SCHEMATIC)

Figure 3-6

with the balanced mixer is the prevention of cross-radiation between the local oscillator and the EPR signal. This is because the E and H-plane arms are uncoupled. [5]

(2) Local Oscillator: The local oscillator, a Varian Associates X-13 klystron, is used to generate a reference signal. The characteristics of the X-13 include the following parameters: The oscillation mode is approximately 40 MHz wide with a total mechanical tuning range of 8.1 to 12.4 GHz. The power output for a matched load is 100 milliwatts at 9.3 GHz.

(3) Mixer-preamplifier: The mixer-preamplifier completes the first detector section of the superheterodyne receiver. The amplifier that was chosen is the LEL 31BPP. It consists of four stages of tuned amplification having an eight megacycle bandwidth, providing most of the signal amplification and selectivity, and serves as a buffer amplifier for the following components of the receiver. [10]

(4) Amplifier: An LEL 301B93 was chosen as the i.f. amplifier. This is a broad-band unit consisting of seven stagger-tuned amplifiers, its function being additional amplification of the coherent signal and to provide for three signal outputs at high impedance: phase detected, video, and i.f. output.

(5) Discriminator: The discriminator, LEL 32B93, provides automatic frequency control. The output of this unit is a dc voltage whose value depends on the difference between the actual i.f. and 30 MHz. The sensitivity of the signal is determined by the narrow-band, tuned amplifiers just prior to the detected output of the discriminator. The dc voltage is then applied to the reflector of the local oscillator to maintain the i.f. at 30 MHz.

Some of the more important parameters that determine the overall operation of the superheterodyne receiver are: (1) sensitivity, which is determined by finding the input power or voltage that is necessary to obtain a standard output, usually the output to a fifty ohm load; (2) selectivity, the characteristic that determines the extent to which the receiver is capable of distinguishing desired signals from signals at other frequencies; (3) fideltiy, the ability to reproduce a modulated signal, determined by using a resistor as the output load impedance; (4) noise figure, which is the ratio of the receiver noise with no signal to the noise of an ideal receiver. [10] Perhaps the most important of the parameters is the noise figure since this is a measure of the smallest input signal that can be distinguished.

A Hewlett Packard noise figure meter, Model 342A, was used to measure the noise figure for this receiver. The noise source was a Hewlett Packard noise tube, Model 349A, an X-band neon tube. The noise tube signal is applied directly to the balanced mixer and the output signal is taken from the last stage of the i.f. amplifier and used as the input to the noise figure meter. Since the gas tube output is the standardization source for the meter, the amount of return signal from the i.f. amplifier is then the measure of the amplitude of the amplifier noise that is generated. Three of the parameters that affect the noise figure are local oscillator tuning, crystal current, and the balanced mixer's efficiency of operation.

The noise figure was determined to be 19.5 db. The necessary crystal current to obtain this lowest noise figure was established to be 0.4 ma. This corresponds to a local oscillator input of 0.63 milliwatts, or -22 db from the power output of the X-13 klystron.

Measurements for selectivity and fidelity were not observed due to the nature of the spectrometer. There is essentially only one frequency at which the system operates, hence, the noise figure is the only parameter that is of significant importance.

CHAPTER IV

EXPERIMENTAL

In the first section we describe the technique involved in operation of the pulsed EPR spectrometer. The second section shows the waveforms of the detected signal at three locations, the output from the microwave diode switch, the signal input to the superheterodyne receiver, and the 30 MHz i.f. signal output of the mixer-preamplifier.

I. OPERATIONAL TECHNIQUE

For the pulsed EPR spectrometer that was constructed, the procedure for its use involves the elementary technique of saturating the spin system and observing the resulting recovery of the spins on an oscilloscope. For saturation, we apply a large microwave pulse, implying that H_1 is large, and keep this signal "on" for a time $t>>T_1$. The EPR signal will then decay to zero when observed on an oscilloscope, and the rate of decay is given by a time constant proportional to W^{-1}, the reciprocal of the stimulated transistion probability per unit time. When the pulse of microwave energy is turned "off" (in a time much shorter than T_1), the signal buildup appears as a rising exponential with time constant T_1, the spin lattice relaxation time. (Of course, $W^{-1}<<T_1$ or no saturation will occur.) A time sequence of the observed signal would appear as indicated in Figure 4-1. The time t_1 is when the pulse is applied and t_2 is the time when the pulse is turned off.

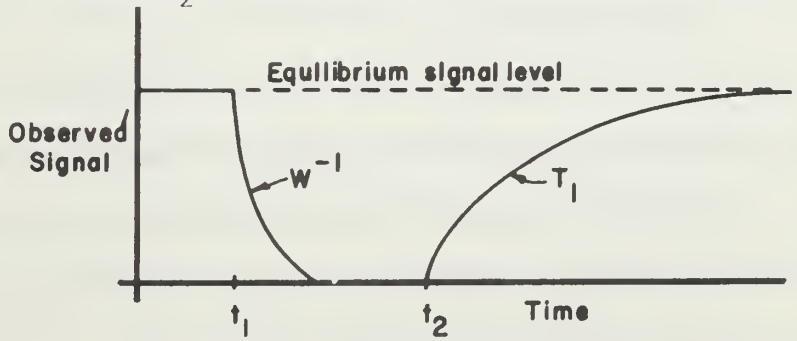

SATURATION AND RECOVERY OF A SPIN SYSTEM

Figure 4-1

As one can see from Figure 4-1, the receiver recovery time must be less than T_1, the quantity that is being measured or the recovery of the signal cannot be observed. Hence, the most important parameter associated with the spectrometer is the superheterodyne receiver recovery time, τ, whose measured value is 0.12 microseconds or roughly the reciprocal of the bandwidth of the receiver (see Figure 4-4). As an experimental criterion, the shortest T_1 that can be measured with confidence is approximately 3 τ. Therefore, the shortest T_1 that can be measured with this spectrometer is on the order of 0.4 microseconds. (Further discussions of pulsed microwave spectroscopy may be found in Dicke and Romer (1955).) [6]

In order to utilize the spectrometer, the following procedures are recommended:

(1) Ordinary precautions concerning the Varian Associates V4200 console must be observed. [9] This includes items such as setting the AFC selector to "off" and placing maximum attenuation in the microwave circuit to avoid crystal damage.

(2) Allow sufficient warm-up time to avoid instabilities that are caused by thermal fluctuations. This takes from four to six hours due to the oil bath cooling for the klystrons.

(3) The room temperature must be held reasonably constant with a minimum of circulation so that gross errors caused by thermal fluctuations are avoided in both the thermistor and the reference cavity that is used for the Pound Stabilizer.

(4) Since the sample cavity is tuned for critical coupling, the slide screw tuner is adjusted in the following manner:

(a) Insert the probe to a depth such that a leakage current is perceptible.

(b) Position the probe along the guide to obtain a maximum leakage current.

(c) Adjust the probe insertion so that the leakage is about one μamp. This corresponds to about one microwatt of microwave power.

(5) Superheterodyne receiver:

(a) Turn "on" the power to the LEL Amplifiers prior to applying power to the local oscillator. This avoids the possibility of the X-13 reflector becoming positive with respect to the cathode or beam.

(b) Once thermal stability has been achieved, set the frequency of the local oscillator to 30 MHz less than the sample cavity frequency. This is done so that the AFC of the superheterodyne receiver will maintain the 30 MHz i.f.

(6) Determine the proper field strength for H_o and turn "on" the dc magnet.

(7) Check the signal output from the receiver. If it is saturated;

(a) increase the attenuation at the input of the receiver. If this is not sufficient,

(b) decrease the probe depth of the slide-screw tuner to reduce the leakage current.

(8) Fine adjust the dc magnet to observe the resonance.

(9) Adjust the Hewlett Packard 243A pulse generator for the proper values of pulse height, duration and repetition rate.

(10) Observe the relaxation time T_1 on any fast rise oscilloscope.

II. SIGNAL WAVEFORMS

The following waveforms were obtained with a Polaroid Land camera attached to the face of a Tektronix 545 oscilloscope modified with a type CA plug-in unit to convert it to a dual trace oscilloscope. Figure 4-2 shows the waveform of the microwave signal from the output of the diode switch. Figure 4-3 displays the waveform of the signal input to the receiver and Figure 4-4 shows the envelope of the 30 MHz i.f. signal out of the preamplifier. In all cases the lower trace is the direct output of the Hewlett Packard 214A pulse generator. The parameters for this signal are: (1) pulse length 1 microsecond; (2) amplitude -8 volts; and (3) pulse repetition rate 4 KHz. In all cases, the polarity of the pulse generator was such that microwave power was switched on during the pulse. A foreward bias of 1.5 volt was applied to the diode gate so that the microwave power was reduced by approximately 30 db in the absence of the 1 microsecond pulse.

The receiver response time, τ, was measured directly from the approximately exponential decay at the trailing edge of the 30 MHz envelope shown in Figure 4-4.

The waveforms for the signal from various locations demonstrate the limitation and capability of the pulsed EPR spectrometer that was constructed. The anomaly of over-shoot, on both the leading and trailing edges of the pulse, is caused by an impedance mismatch when using the

oscilloscope for crystal detected outputs. The slight overshoot that is evident on the 30 MHz i.f. envelope is caused by the receiver reactive elements. This overshoot of signal is desirable because it indicates maximum receiver response, just as a control circuit is at maximum sensitivity when the circuit is tuned slightly below critical damping. The 0.1 microsecond time lag for the receiver signal that is evident in Figure 4-4 is caused entirely by the reactive elements in the receiver. An analysis, considering the tuned circuits in the receiver as cascaded filters, will yield expressions to compute values for the expected time lag of signal appearance. [10] However, since this time lag is a constant, it does not affect the measurement of T_1.

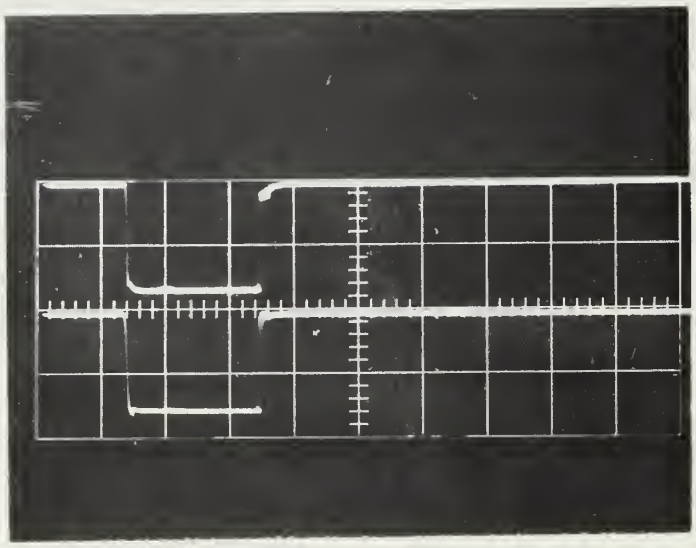

DIODE SWITCH OUTPUT VERSUS TIME

Figure 4-2

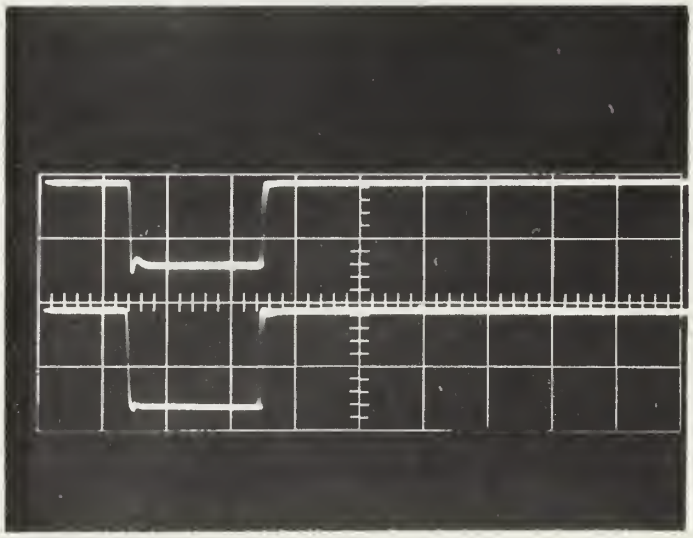

SIGNAL INPUT TO RECEIVER VERSUS TIME

Figure 4-3

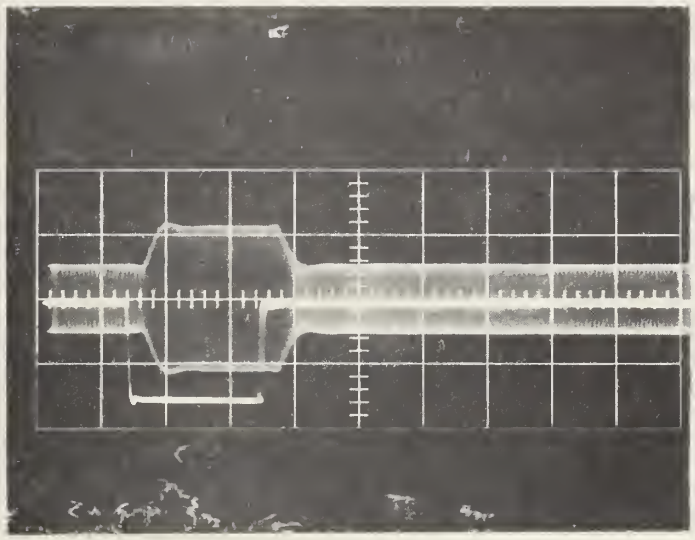

ENVELOPE OF 30 MHz SIGNAL VERSUS TIME

Figure 4-4

BIBLIOGRAPHY

1. Pake, G.E. Paramagnetic Resonance, New York: W.A. Benjamin, Inc., 1962.

2. Eisberg, Robert Martin. Fundamentals of Modern Physics, New York: John Wiley and Sons, Inc., 1963.

3. Siegman, A.E. Microwave Solid-state Masers, New York: McGraw-Hill Book Company, 1964.

4. Slichter, Charles P. Principles of Magnetic Resonance, New York: Harper and Row, 1963.

5. Collins, Robert E. Foundations for Microwave Engineering, New York: McGraw-Hill Book Company, 1966.

6. Poole, Charles P., Jr. Electron Spin Resonance, New York: Interscience Publishers, 1967.

7. Montgomery, Carol G. Technique of Microwave Measurements, New York: McGraw-Hill Book Company, 1947.

8. Ginzton, Edward L. Microwave Measurements, New York: McGraw-Hill Book Company, 1957.

9. Operating Instructions, Publication Number 87-114-200, Palo Alto: Varian Associates.

10. Terman, Frederick Emmons. Electronic and Radio Engineering. Fourth edition. New York: McGraw-Hill Book Company, 1955.

APPENDIX A

QUANTUM MACHANICAL DESCRIPTION OF MAGNETIC DIPOLES IN A STATIC FIELD

First begin with the Schroedinger equation:

$$\nabla^2\Psi + \frac{2m}{\hbar^2}(E - V)\Psi = 0 ,$$

where ∇^2 is the Laplacian, Ψ = the wave function to describe the system, m = mass of the particle, $\hbar = h/2\pi$ = Planck's constant times $1/2\pi$, E = total energy, and V = potential energy. If $V = V(r,\theta, \phi, t)$, then,

$$\nabla^2\Psi - \frac{2m}{\hbar^2} V(r, \theta, \phi, t) = i\hbar \frac{\partial}{\partial t}\Psi ,$$

where the energy operator $E \equiv \frac{\hbar}{i}\frac{\partial}{\partial t}\Psi$. Assume (r, θ, ϕ, t) can be separated into a product of its space and time co-ordinated, i.e.,

$$\Psi(r, \theta, \phi, t) = \psi(r, \theta, \phi)f(t) ,$$

then f(t) is given by $f(t) = \exp(-iEt/\hbar)$. Assuming that spin variables may be separated from space and time co-ordinates, we now transform into a function of spin and time variables:

$$\Psi_{I,m}(t) = U_{I,m}\exp(-iE_m t/\hbar) ,$$

where $I = |\vec{I}|$, the spin magnetic moment, and m = I, I-1, ..., -I, the eigenvalues of the component of spin along the static field or H_o axis and $E_m = -\gamma\hbar H_o m$. The most general time dependent solution is therefore:

$$\Psi_{I,m}(t) = \sum_{m=-I}^{+I} C_m U_{I,m}\exp(-iE_m t/\hbar) ,$$

where C_m is a complex constant and $|C_m|^2$ is the probability for the system to be in a state m. Now, we may compute the expectation value

of any observable by means of $\Psi_{I,m}$, i.e., let $\langle O(t)\rangle$ be the expectation value of any observable and O_{op} be the operator for this observable. Then,

$$\langle O(t)\rangle = \int_{-\infty}^{\infty} \Psi^*(t) O_{op} \Psi(t) d\tau \ ,$$

and τ is the pseudo-variable of integration to indicate integration over spin space.

As an illustration, we will compute the expectation value of the x-component of magnetization, $\langle \mu_x(t)\rangle$. First, define $E_{m'} - E_m = \hbar\omega_{m',m}$ and $\mu = \gamma\hbar I$, then,

$$\langle \mu_x(t)\rangle = \gamma h C^*_{m'} C_m \int [U^{**}_{I,m'} (I_x)_{op} U_{I,m} d\tau] \exp(i\omega_{m',m} t) \ ,$$

where $(I_x)_{op}$ is the operator for the x-component of magnetization. Here it is convenient to introduce the raising and lowering operators, I^+ and I^- that are defined by:

$$I^+ = I_x + iI_y \ ,$$

and

$$I^- = I_x - iI_y \ .$$

The operators are called "raising" and "lowering" operators because of the effect they produce when they operate on a function:

$$I^+ U_{I,m} = \sqrt{I(I+1) - m(m+1)} \quad U_{I,m+1} \ ,$$

and

$$I^- U_{I,m} \quad \sqrt{I(I+1) - m(m-1)} \quad U_{I,m-1} \ .$$

Hence,

$$\int U^*_{I,m'}(I^+)U_{I,m} = \sqrt{I(I+1) - m(m+1)} \int U^*_{I,m'}U_{I,m}$$

$$= \sqrt{I(I+1) - m(m-1)}\ \delta_{m',m+1} \ ,$$

and similarly,

$$\int U^*_{I,m'}(I^-)U_{I,m} = \sqrt{I(I+1) - m(m+1)}\ \delta_{m',m+1} \ ,$$

due to orthogonality of the spin wave function.

If we take a simple two-level system where $I = \frac{1}{2}$, then $m = \pm\frac{1}{2}$ and defining $|\omega_{-\frac{1}{2},\frac{1}{2}}| = |(E_{-\frac{1}{2}} - E_{\frac{1}{2}})/\hbar| = \gamma H_o = \omega_o$, the result is:

$$\langle\mu_x\rangle = \gamma\hbar/2\ \{C^*_{\frac{1}{2}}C_{-\frac{1}{2}}\int[U^*_{\frac{1}{2},-\frac{1}{2}}(I^+)U_{,-}\ d\tau]\exp(+i\omega_o t) +$$

$$C^*_{-\frac{1}{2},\frac{1}{2}}\int[U^*_{\frac{1}{2},\frac{1}{2}}(I^-)U_{,}\ d\tau]\exp(-i\omega_o t)\} \ .$$

Note that;

$$\int U^*_{I,m'}(I_x)U_{I,m}d\tau = [\int U^*_{I,m}(I_x)U_{I,m'}d\tau]^* \ .$$

Hence:

$$\langle\mu_x\rangle = \gamma\hbar/2C^*_{\frac{1}{2}}C_{-\frac{1}{2}}\sqrt{\tfrac{1}{2}(\tfrac{1}{2}+1) - (-\tfrac{1}{2})(-\tfrac{1}{2}+1)}\exp(i\omega_o t) + \text{complex conjugate}$$

$$= \gamma\hbar/2C^*_{\frac{1}{2}}C_{-\frac{1}{2}}\exp(+i\omega_o t) + \text{complex conjugate.}$$

For convenience, define new variables such that C_i is expressed as a function of real quantities. Choose a and b to be real positive numbers and two other real quantities, α and β that may be either positive or negative. Thus;

$$C_{\frac{1}{2}} = a\exp(i\alpha) \ ,$$

and,

$$C_{-\frac{1}{2}} = b \exp(i\beta) \ .$$

Notice that in order to retain proper normalization, a and b are chosen so that $a^2 + b^2 = 1$. Therefore;

$$\langle \mu_x \rangle = \gamma\hbar/2ab[\exp(-i(\alpha - \beta - \omega_o t)) + \exp(i(\alpha - \beta - \omega_o t))] \ ,$$

or,

$$\langle \mu_x \rangle = \gamma\hbar ab \cos(\alpha - \beta - \omega_o t) \ ,$$

and correspondingly,

$$\langle \mu_y \rangle = -\gamma\hbar \ ab \sin(\alpha - \beta - \omega_o t) \ .$$

Now from the relationship;

$$\langle \mu \rangle^2 = [\tfrac{1}{2}\gamma\hbar]^2 = \langle \mu_x \rangle^2 + \langle \mu_y \rangle^2 + \langle \mu_z \rangle^2$$

we find that;

$$\langle \mu_z \rangle = \gamma\hbar[\frac{a^2 - b^2}{2}] \ .$$

Graphically, the preceeding expectation value s for the magnetization are;

$$\langle \mu_x \rangle = \langle \mu \rangle \sin\theta \cos\phi \ ,$$

$$\langle \mu_y \rangle = \langle \mu \rangle \sin\theta \sin\phi \ ,$$

$$\langle \mu_z \rangle = \langle \mu \rangle \cos\theta \ ,$$

where

$$|\langle \mu \rangle| = \tfrac{1}{2}\gamma\hbar \ ,$$

and

$$\cos\theta = a^2 - b^2 \ .$$

Then, when trigonometric identities are substituted, the following results are obtained:

$$\tfrac{1}{2}\sin\theta\cos\phi = ab\cos(\alpha - \beta - \omega_o t) ,$$

$$\tfrac{1}{2}\sin\theta\sin\phi = ab\sin(\alpha - \beta - \omega_o t) ,$$

$$\tfrac{1}{2}\sin\theta = ab.$$

Thus, one can say that;

$$\cos\phi = \cos(\alpha - \beta - \omega_o t) ,$$

or that,

$$\phi = (\alpha - \beta - \omega_o t) .$$

The physical significance is that the expectation value of the operator acts as does a vector of length $\gamma\hbar/2$ whose direction is given by the spherical co-ordinates, θ and ϕ . If the orientation is known at a given time, t, then the orientation can be found at some later time t_1 from the above equation and one immediately finds that $\langle\mu\rangle$ precesses about H_o with angular velocity ω_o in the negative ϕ direction. Thus we see that the quantum mechanical description of the expectation value of magnetization of a collection of spins is equivalent to the classical description of the motion of a magnetic moment in an external field.

INITIAL DISTRIBUTION LIST

		No. Copies
1.	Defense Documentation Center Cameron Station Alexandria, Virginia 22314	20
2.	Library Naval Postgraduate School Monterey, California 93940	2
3.	Commander Naval Ordnance Systems Command Navy Department Washington, D. C. 20360	1
4.	Professor Gordon E. Schacher Department of Physics Naval Postgraduate School Monterey, California 93940	1
5.	Professor John R. Neighbours Department of Physics Naval Postgraduate School Monterey, California 93940	1
6.	LT Homer S. Nakayama USS Joseph Strauss (DDG-16) Fleet Post Office San Francisco, California 96601	2

DOCUMENT CONTROL DATA - R & D

Security classification of title, body of abstract and indexing annotation must be entered when the overall report is classified)

1 ORIGINATING ACTIVITY (Corporate author)
Naval Postgraduate School
Monterey, California 93940

2a. REPORT SECURITY CLASSIFICATION
Unclassified

2b. GROUP

3 REPORT TITLE

Construction of a Pulsed Superheterodyne EPR Spectrometer

4 DESCRIPTIVE NOTES (Type of report and inclusive dates)
Masters thesis - June 1968

5 AUTHOR(S) (First name, middle initial, last name)

Homer S. Nakayama Lieutenant United States Navy

6. REPORT DATE	7a. TOTAL NO. OF PAGES	7b. NO. OF REFS
June 1968	51	10

8a. CONTRACT OR GRANT NO.

b. PROJECT NO

c.

d.

9a. ORIGINATOR'S REPORT NUMBER(S)

9b. OTHER REPORT NO(S) (Any other numbers that may be assigned this report)

10. DISTRIBUTION STATEMENT

[redacted]

11. SUPPLEMENTARY NOTES

12. SPONSORING MILITARY ACTIVITY
Naval Postgraduate School
Monterey, California

13. ABSTRACT

The general theory of electron paramagnetic resonance (EPR) is discussed to present a background for the Bloch equations, hence explaining the phenomena of relaxation times in paramagnetic materials. Then, the details of construction of the pulsed superheterodyne EPR spectrometer are discussed in which the characteristics and functions of the components are specified. Procedures for its use in the measurement of T_1 are indicated and waveforms from various locations are presented to show the limitation of the pulsed EPR spectrometer that was constructed.

14 KEY WORDS	LINK A		LINK B		LINK C	
	ROLE	WT	ROLE	WT	ROLE	WT
Pulsed Superheterodyne EPR Spectrometer						
Electron Paramagnetic Resonance						
Measurement of Relaxation Times						